

Estimation of sensible heat, water vapor, and CO₂ fluxes using the flux-variance method

Cheng-I Hsieh · Mei-Chun Lai · Yue-Joe Hsia ·
Tsang-Jung Chang

Received: 23 September 2007 / Revised: 20 February 2008 / Accepted: 21 February 2008 / Published online: 1 April 2008
© ISB 2008

Abstract This study investigated the flux-variance relationships of temperature, humidity, and CO₂, and examined the performance of using this method for predicting sensible heat (H), water vapor (LE), and CO₂ fluxes (F_{CO₂}) with eddy-covariance measured flux data at three different ecosystems: grassland, paddy rice field, and forest. The H and LE estimations were found to be in good agreement with the measurements over the three fields. The prediction accuracy of LE could be improved by around 15% if the predictions were obtained by the flux-variance method in conjunction with measured sensible heat fluxes. Moreover, the paddy rice field was found to be a special case where water vapor follows flux-variance relation better than heat does. However, the CO₂ flux predictions were found to vary from poor to fair among the three sites. This is attributed to the complicated CO₂ sources and sinks distribution. Our results also showed that heat and water vapor were transported with the same efficiency above the grassland and rice paddy. For the forest, heat was transported 20% more efficiently than evapotranspiration.

Keywords Flux-variance method · Evapotranspiration · CO₂ flux · Rice paddy

Introduction

Surface fluxes of sensible heat, water vapor, and CO₂ in the atmospheric boundary layer are important parameters for the understanding of the interactions and energy/mass transport processes between land-surface and atmosphere. Many methods have been developed to quantify these fluxes, including the eddy-covariance method, flux-gradient method, dissipation method, flux-variance method, and surface renewal method. Among these methods, the flux-variance method is the least difficult one since it requires only the variance measurement of the scalar at one level (e.g., Padro 1993; Wesson et al. 2001; Castellvi and Martinez-Cob 2005) and is especially useful when high frequency wind velocity measurements are not available. For example, for calculating sensible heat fluxes, the flux-variance method only needs a thermocouple, while the eddy-covariance method requires a sonic anemometer. The flux-variance method was based on Monin-Obukhov similarity theory (MOST) and first proposed by Tillman (1972) to estimate sensible heat flux. This method was later examined for quantifying water vapor flux and its performance was found to vary from poor (e.g., de Bruin et al. 1993; Asanuma and Brutsaert 1999) to good (e.g., Weaver 1990; Andreas et al. 1998). Recently, Castellvi and Martinez-Cob (2005) applied the flux-variance method to estimate surface-layer and mixed-layer sensible heat fluxes. They found that this method could reproduce the sensible heat fluxes in both layers, but the accuracy of surface-layer estimation is twice of that for mixed-layer.

Though the flux-variance method has been widely used and examined for determining sensible and water vapor fluxes under different surface types and atmospheric stability conditions (Wesely 1988; Weaver 1990; Lloyd et al. 1991; Katul et al. 1995; Hsieh et al. 1996), less

C.-I. Hsieh (✉) · M.-C. Lai · T.-J. Chang
Department of Bioenvironmental Systems Engineering,
National Taiwan University,
Taipei 10617, Taiwan
e-mail: hsieh@ntu.edu.tw

Y.-J. Hsia
Institute of Natural Resources, National Dong Hwa University,
Hualien 97401, Taiwan

attention has been paid to examining this method for estimating CO₂ flux. Ohtaki (1985) examined the flux-variance relations of sensible heat, water vapor, and CO₂ over two wheat fields in Japan. He concluded that these three scalars have similar Monin-Obukhov flux-variance relations. This also implies that the flux-variance method might be extended for quantifying CO₂ flux. However, Williams et al. (2007) pointed out that seasonal changes can produce a surface heterogeneity in the scalar source/sink field, thus weakening the similarity relationship, particularly in the case of CO₂. Using the experiment above a suburban area, Moriwaki and Kanda (2006) also indicated that the differences of turbulent transfer between heat and both water vapor and CO₂ were probably due to the heterogeneity in the source distribution of scalars. Hence, more studies are needed for establishing the flux-variance relation for CO₂.

It is the importance of developing and testing simple methods (like the flux-variance method) for determining surface fluxes between land and atmosphere that motivates this study. The purposes of this study are to determine, with MOST, the flux-variance relations of sensible heat, water vapor, and CO₂ above different surface types, and to examine its performance in predicting these surface fluxes. For the purposes of this study, experiments were carried out above three different surfaces: a temperate humid grassland in Cork, Ireland; an irrigated subtropical paddy rice field in Taipei, Taiwan; and a natural-regenerated yellow cypress forest in Ilan, Taiwan. These three sites represent surface roughness for momentum and scalars from smooth to rough.

Materials and methods

Flux-variance method is based on Monin-Obukhov similarity theory. For the unstable atmospheric surface layer over a homogeneous and flat surface, the normalized standard deviation of a scalar quantity, X , can be expressed as a function of the Monin-Obukhov stability parameter, ζ ,

$$\frac{\sigma_x}{X_*} = C_x(\zeta)^{-1/3} \quad (1)$$

where σ_x is the standard deviation of the scalar quantity, X , C_x is a similarity constant, and X_* is a scalar scale defined as $X_* = \overline{w'x'}/u_*$; $\overline{w'x'}$ represents the turbulent flux of the scalar, w' and x' are the fluctuation parts of the vertical velocity W and scalar X , respectively, the over bar denotes time average, the prime denotes deviation from the mean, and u_* is the friction velocity. In Eq. (1), the atmospheric stability parameter, ζ , is defined as $\zeta = -(z-d)/L$, where z is the measurement height, d is the zero-plane displacement ($\approx .65$ h; h is the canopy height, Campbell and Norman,

1998), and L is the Obukhov length defined as $L = -Tu_*^3/.kgw'T'$; T is the air temperature, k ($= 0.4$) is the von Karman constant; and g is the gravitational acceleration. Notice that a $-1/3$ power law exists in Eq. (1) for any scalar quantity.

In this study, the scalar quantities of interest are temperature, water vapor, and CO₂; hence, by Eq. (1) we have:

$$\frac{\sigma_T}{T_*} = C_T(\zeta)^{-1/3} \quad (2)$$

$$\frac{\sigma_q}{q_*} = C_q(\zeta)^{-1/3} \quad (3)$$

$$\frac{\sigma_{CO_2}}{CO_{2*}} = C_{CO_2}(\zeta)^{-1/3} \quad (4)$$

where the sub-indexes T , q and CO_2 denote temperature, absolute humidity, and carbon dioxide concentration, C_T , C_q , and C_{CO_2} are flux-variance similarity constants, and T_* , q_* , and CO_{2*} are scales defined as $\overline{w'T'}/u_*$, $\overline{w'q'}/u_*$, and $-\overline{w'CO_2'}/u_*$, respectively.

By substituting L with its definition in Eq. (2), (3), and (4), the fluxes of sensible heat (H), latent heat (LE), and carbon dioxide (F_{CO_2}) can be expressed as the following:

$$H = \rho C_p \overline{w'T'} = \rho C_p \left(\frac{\sigma_T}{C_T} \right)^{3/2} \left(\frac{kg(z-d)}{T} \right)^{1/2} \quad (5)$$

$$LE = L_v \overline{w'q'} = L_v \frac{\sigma_q}{C_q} \left(\frac{kg\sigma_T(z-d)}{C_T T} \right)^{1/2} \quad (6)$$

$$F_{CO_2} = \overline{w'CO_2'} = - \frac{\sigma_{CO_2}}{C_{CO_2}} \left(\frac{kg\sigma_T(z-d)}{C_T T} \right)^{1/2} \quad (7)$$

where ρ (≈ 1.225 mol m⁻³) is the mean air density, C_p (≈ 29.3 J mol⁻¹ K⁻¹) is the specific heat capacity of air, L_v ($\approx 2,450$ J g⁻¹) is the latent heat of vaporization. By Eq. (5), H can be conveniently determined from σ_T only. Also, by Eq. (6) and (7), LE and F_{CO_2} can be predicted with σ_T and σ_q , and σ_T and σ_{CO_2} , respectively. Hence, by Eq. (5) to (7), measurements at only one height are sufficient for estimating sensible heat, water vapor, and CO₂ fluxes under unstable conditions.

For using Eq. (5) to (7) to estimate H , LE , and F_{CO_2} , the flux-variance similarity constants C_T , C_q , and C_{CO_2} need to be determined a priori. In this study, the field data measured from the three different sites were divided into two parts. The first part of the measurements was used to determine the similarity constants. The second half of the data was

Table 1 Summary of site characteristics and eddy-covariance measurement at three sites

Ecosystem	Grassland	Paddy rice field	Forest
Date of experiment	1 Jan ~ 31 Dec 2002	26 Sep 2006 ~ 18 May 2007	1 Apr 2005 ~ 31 Dec 2006
Elevation (m)	~ 200	< 20	~1,670
Site latitude and longitude	52°8'24"N, 8°39'36"W	24°57'41"N, 121°31'38"E	24°35'27"N, 121°29'56"W
Climate	Temperate	Subtropical monsoon	Warm temperate
Annual precipitation (mm)	1,470	2,500	4,000
Annual mean temperature (°C)	11.5	23	13
Canopy height (m)	0.1 ~ 0.45	0.5 ~ 0.8	10.3
Measurement height (m)	10	2	24
Surface roughness (m)	0.03	0.06	1
Sonic anemometer	Young 81000, R M Young	CSAT3, Campbell Scientific	Young 81000V, R M Young
CO ₂ /H ₂ O analyzer	LI 7500, Li-cor	LI 7500, Li-cor	LI 7500, Li-cor
Separation distance between sonic anemometer and CO ₂ /H ₂ O analyzer	15 cm	15 cm	15 cm

then used to examine the performance of flux-variance method for predicting sensible heat, water vapor, and CO₂ fluxes.

Experiments

Three experiments of eddy-covariance measurements were carried out for examining the performance of flux-variance method over smooth, mid-rough, and rough surfaces. Details of the experiments were described below and a brief summary of the three sites and instrumentations is listed in Table 1. Pictures for the experimental set-up of the three sites were also shown in Figs. 1, 2 and 3.



Fig. 1 Experimental set-up for the grassland site

Grassland experiment

This experiment was conducted over a temperate, humid, and flat grassland in Cork County in southwest Ireland (52° 8'24"N, 8°39'36"W). The fetch in the main wind direction was 2.0 km and the shortest fetch was 1.2 km. Data collected in the whole year of 2002 was used in this study. The grassland type is pasture and meadow, and the dominant plant species is perennial ryegrass. The grass height in the grazing fields varied from 0.1 to 0.2 m and had a maximum of 0.45 m in the harvested fields. The surface roughness of this site was around 0.03 m, determined from the logarithmic mean wind equation under neutral conditions with measured mean wind velocities and friction velocities (Hsieh et al. 2005).

A three-dimensional sonic anemometer (RM Young 81000) was used to measure the wind vector and virtual



Fig. 2 Experimental set-up for the paddy rice field



Fig. 3 Experimental set-up for the forest Site

potential temperature, converted from the speed of sound. And CO_2 and H_2O concentrations were measured with an open-path $\text{CO}_2/\text{H}_2\text{O}$ infrared gas analyzer (LI7500, Li-Cor) placed at a distance of 15 cm from the center of the anemometer. Both of the anemometer and the gas analyzer were positioned at the top of a 10-m tower. The raw data, measured and averaged at 10 Hz and 30 min, respectively, were collected with a data-logger and then transmitted to a computer. Details about this grassland and experiment can also be found in Jaksic et al. (2006).

Paddy rice field experiment

This experiment was conducted from 26 September 2006 to 18 May 2007 over an irrigated paddy rice field at An-Kang experimental farm of National Taiwan University, Taipei, Taiwan. (The vegetation periods for the paddy rice field were from 26 September 2006 to 6 December 2007 and 10 March to 18 May 2007. Only data collected in these periods were used.) The farm site is flat and is located on the outskirts of Taipei city. The fetch along the main wind direction was 0.5 km and the shortest fetch was 0.3 km. This study site has the representative subtropical monsoon climate feature: dry and warm in winter, and wet and hot in summer. The average heights of paddy rice were 0.5 m and 0.8 m for the growing and maturity periods, respectively. The average surface roughness was 0.06 m (determined from the same method mentioned in the Grassland experiment). The rice field was flooded with 2–8 cm depth of water during the growing period.

An eddy-covariance system, consisting of a sonic anemometer (CSAT3, Campbell Scientific) and an open-path $\text{CO}_2/\text{H}_2\text{O}$ infrared gas analyzer (LI7500, Li-Cor), was installed at the height of 2.0 m above the ground to measure the sensible heat, water vapor, and CO_2 fluxes. The sampling frequency for velocities, temperature, humidity, and CO_2 concentration was 10 Hz, and the averaging

period was 30 min. The signals of the measurements were collected with a data-logger and then transmitted to a computer.

Forest experiment

The experiment was carried out above a natural-regenerated yellow cypress plantation in Chi-Lan Mountain, Ilan, Taiwan. The yellow cypress forest area is 374 ha and covers an altitude range between 1,650 and 2,432 m a.s.l., with a homogeneous slope of 15° . The fetch in the main wind directions was 1.8 km and the shortest fetch was 1.0 km. The forest is a typical cypress forest with an average height of 10.3 m. The surface roughness is 1.0 m (determined by the

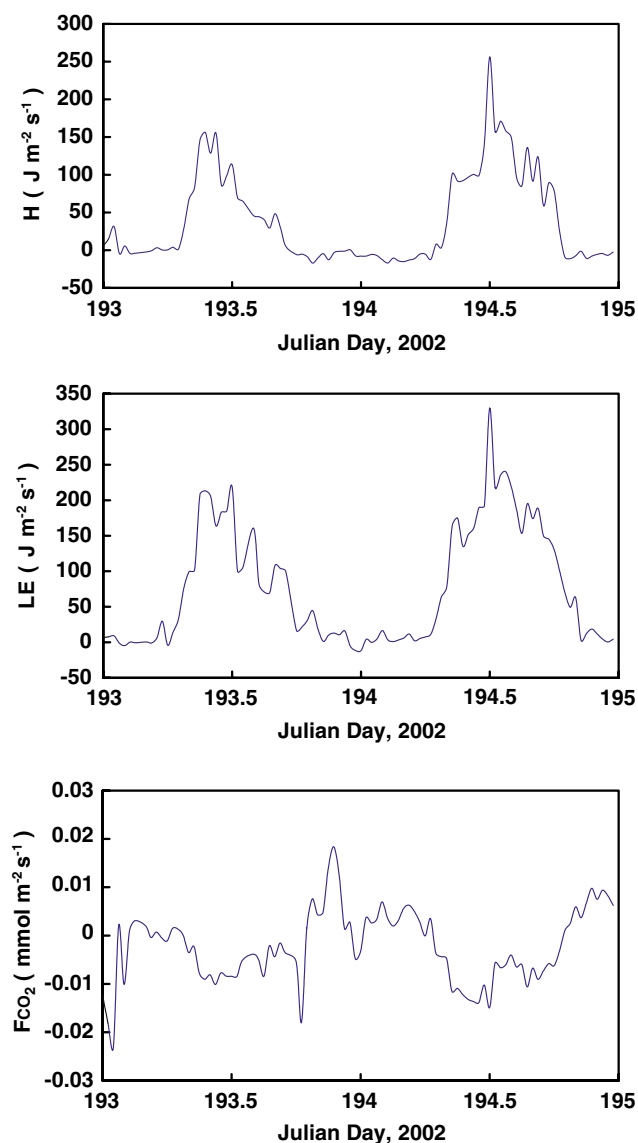


Fig. 4 Typical temporal variations of (*upper panel*) sensible heat, (*middle*) water vapor, and (*lower*) CO_2 fluxes above the grassland

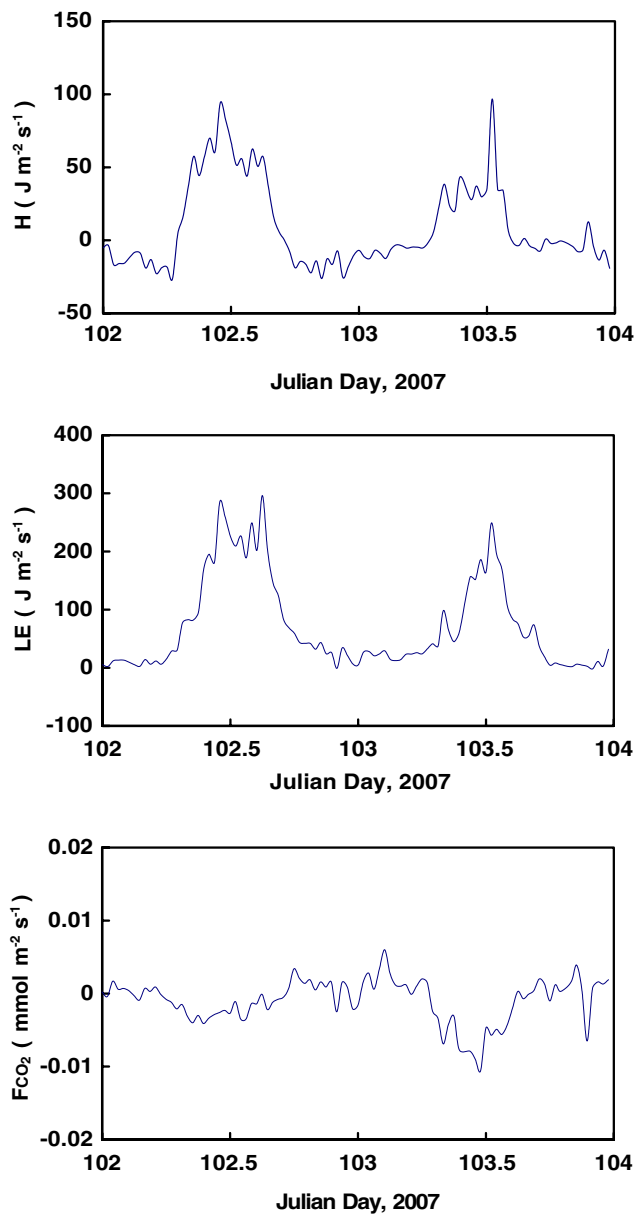


Fig. 5 Typical temporal variations of (*upper panel*) sensible heat, (*middle*) water vapor, and (*lower*) CO₂ fluxes above the paddy rice field

same method in the Grassland experiment). Due to its topography and elevation, the climate is temperate and warm during the whole year. The flux data assembled from April 2005 to December 2006 were used in this study.

The measurements of wind speed and sonic temperature were obtained with a three-dimensional sonic anemometer (RM Young 81000v). The CO₂ concentration and humidity were also measured with LI7500 open-path infrared gas analyzer. The system was mounted on top of a 24-m-tall walk-up tower. Analog signals from the LI7500 were synchronized with the signals of the sonic anemometer and digital data were then transmitted to a ground base computer at 10-Hz sampling rate and 30-min averaging period.

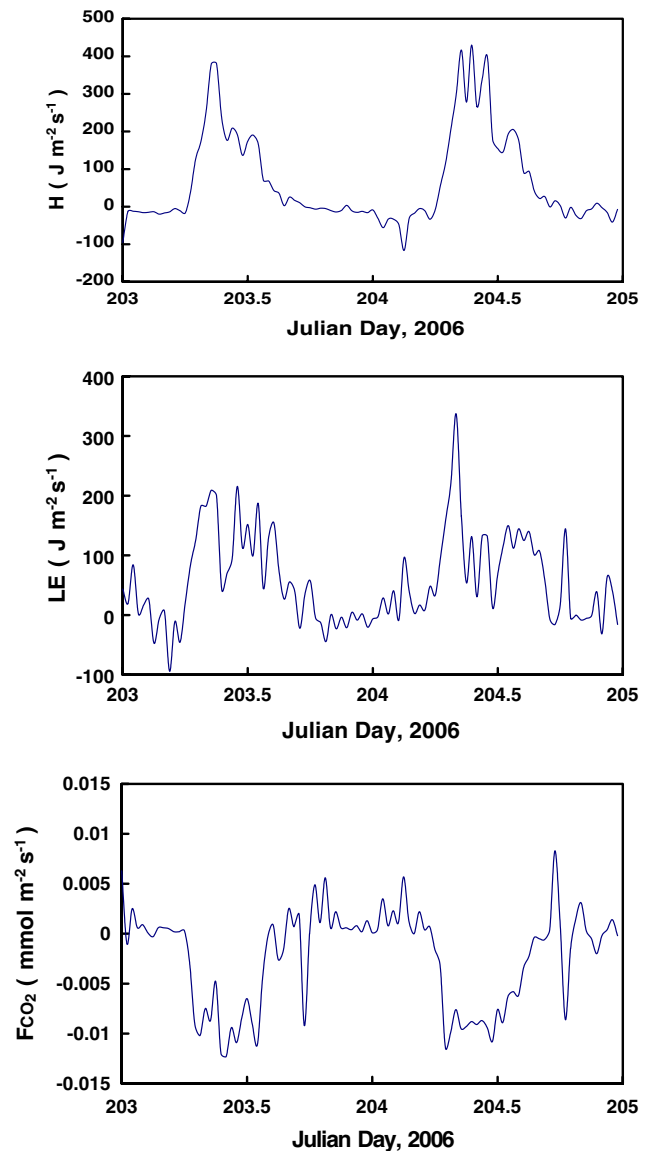


Fig. 6 Typical temporal variations of (*upper panel*) sensible heat, (*middle*) water vapor, and (*lower*) CO₂ fluxes above the forest

Data processing

All the data collected from the three sites were checked and calculated with the following processes:

1. Detrending, despiking, and spectral correction were applied for the flux calculation. Detrending was done by removing the linear trend of the raw data. Spikes outside the ± 3 standard deviation were replaced with the interpolated values. If the number of spikes exceeded 1% of the total number of each measurement run, then this run was abandoned. The spectral correction (frequency filtering) was done following Moore (1986).
2. The x coordinate was double rotated to be along with the mean wind direction; hence, the mean lateral and vertical wind velocity were zero (McMillen 1988). The

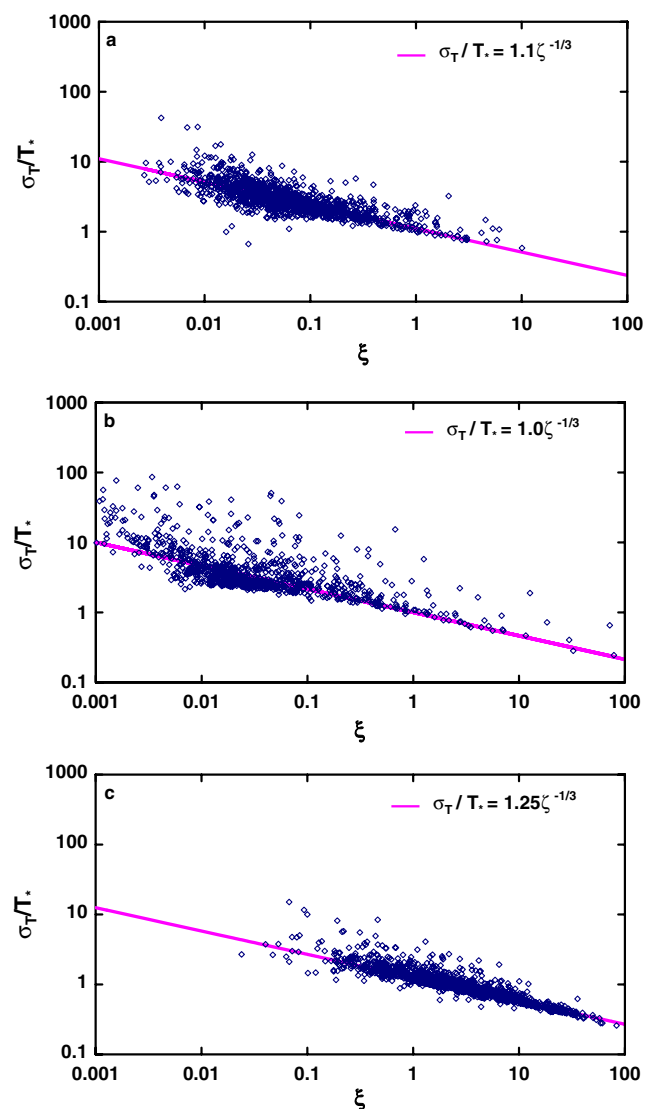


Fig. 7 Normalized standard deviation of temperature (σ_T/T_*) as a function of stability parameter (ξ) for **a** grassland, **b** rice paddy field, and **c** forest

planar fit method (Wilczak et al. 2001) was also used for the coordinate rotation, but no significant difference was found.

3. The Webb, Pearman, and Leuning (WPL) correction was used when calculating water vapor and CO_2 fluxes (Webb et al. 1980), and was also applied to the flux-variance relationships following Detto and Katul (2007).
4. Only data collected under unstable conditions were used for analyzing flux-variance relationships.
5. The stability parameter, $(z-d)/L$, was determined from the eddy-covariance system.
6. Negative CO_2 fluxes denote carbon dioxide uptake by the ecosystems. However, while examining the flux-variance relations and its performance for CO_2

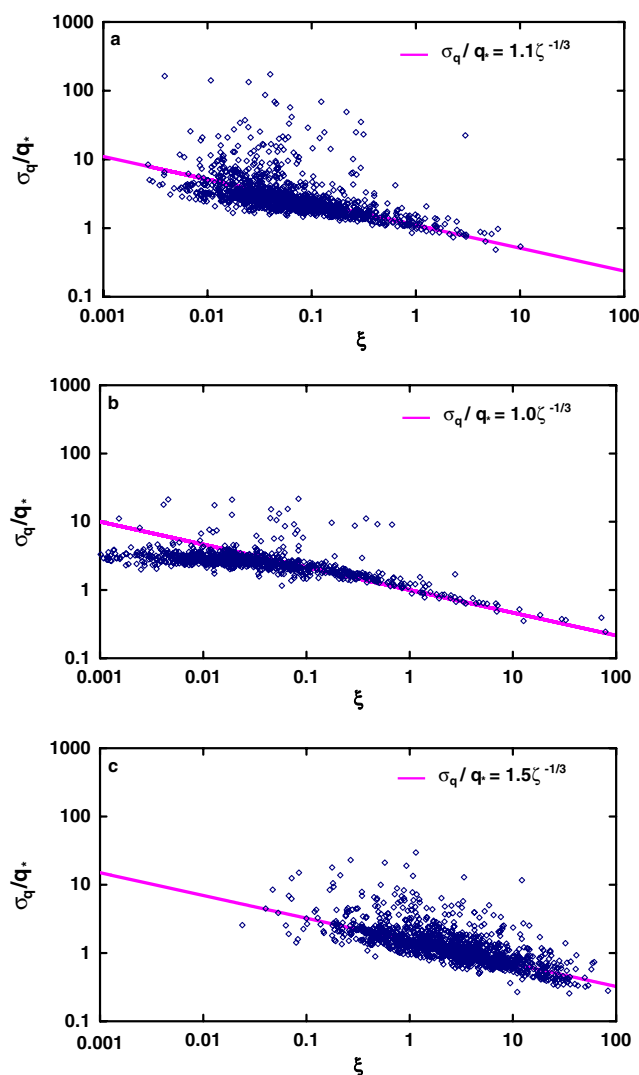


Fig. 8 Normalized standard deviation of water vapor (σ_q/q_*) as a function of stability parameter (ξ) for **a** grassland, **b** rice paddy field, and **c** forest

flux estimation, the negative sign was turned into positive.

7. The positive CO_2 and negative water vapor flux values during unstable situations were considered not acceptable and not used in this study.

Footprint analysis

In this study, the footprint analysis was done using the Hsieh et al. (2000) model. The fetch requirements for the grassland, rice paddy, and forest were found to be 1.0, 0.15, and 0.8 km, respectively. The footprint analysis also showed that, along the mean wind direction, the locations of the maximum source strength for the grassland, rice paddy, and forest were 56, 6.0, and 42 m from the tower, respectively.

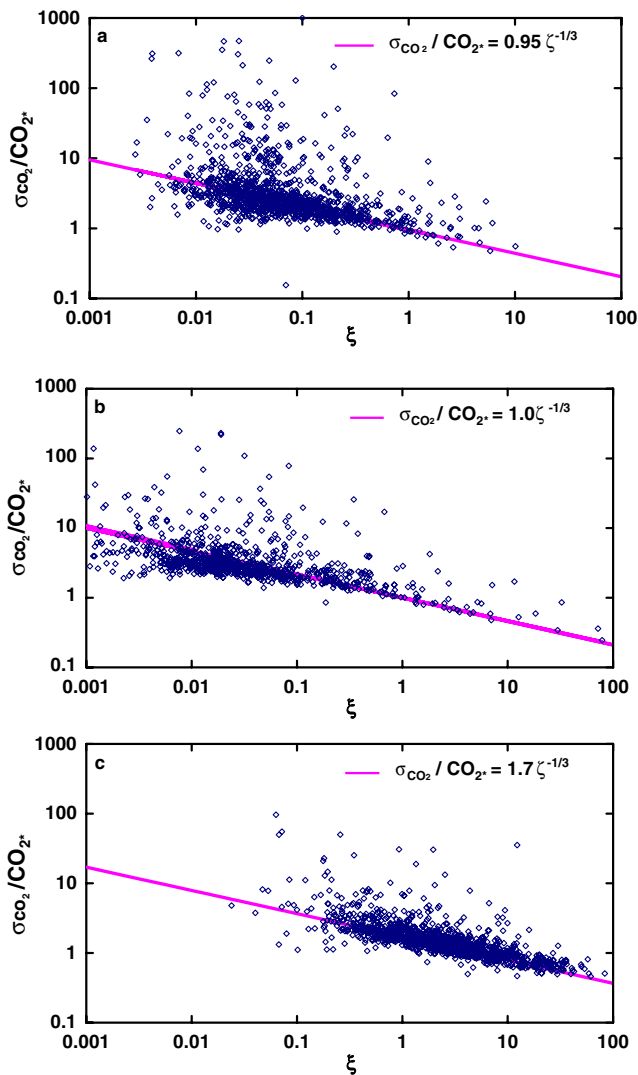


Fig. 9 Normalized standard deviation of CO₂ (σ_{CO_2}/CO_{2^*}) as a function of stability parameter (ξ) for **a** grassland, **b** rice paddy field, and **c** forest

Results and discussion

In this section, we first present the temporal variations of sensible heat, water vapor, and carbon dioxide fluxes above the three ecosystems, then we discuss the flux-variance relations and the performance of flux-variance method in estimating surface fluxes.

Temporal variations of sensible heat, water vapor, and CO₂ fluxes

Figure 4 shows a typical temporal variation of sensible heat, water vapor, and CO₂ fluxes above the grassland for 2 days, from day 193 to 195. It is clear that these three fluxes had their maximum values around noon when the daytime net radiation was high. Also, notice that the water vapor flux was about 30–50% higher than the sensible heat flux, showing that more net radiation energy was used for evapotranspiration from this humid grassland. Figures 5 and 6 are the same as Fig. 4 but for the paddy rice field and forest, respectively. In Fig. 5, the sensible heat fluxes were small and were only half of the latent heat flux above the rice paddy. This was due to the rice paddy being irrigated and the field surface filled with water. However, for the forest, the sensible heat fluxes were twice of the latent heat fluxes (Fig. 6). This demonstrated that much of the net radiation energy was used for surface heating rather than evapotranspiration for the forest site.

As to the CO₂ fluxes, from Figs. 4, 5 and 6, it shows that the forest has the highest CO₂ uptake among these three sites and that its magnitude was about 1.5 times of those for the grassland and rice paddy. Figures 4, 5 and 6 also show that during night-time the respiration rates from these three ecosystems were small compared with the daytime CO₂ uptake. During daytime, when photosynthesis reaction is active, CO₂ assimilation and transpiration are strong since the stomata are open for taking CO₂ and releasing water vapor. During night-time, the stomata are closed, hence CO₂ flux and transpiration are small. The water vapor flux (LE) not only includes the transpiration from the vegetation but also the evaporation from the surface, so it is less affected by the vegetation physiological processes.

Flux-variance relationship for temperature, humidity, and CO₂

Flux-variance relations need to be determined before using the flux-variance method to estimate the surface fluxes (e.g., Weaver 1990; Padro 1993). On the basis of MOST, with (Eq. (2) to (4) and direct eddy-covariance measurements, we determine the flux-variance relations of temperature, humidity, and CO₂. Figure 7 shows the normalized

Table 2 Flux-variance similarity constants for temperature (C_T), humidity (C_q), and carbon dioxide (C_{CO_2}) for the three ecosystems

Ecosystem	C_T	C_q	C_{CO_2}	No. of data points	Date
Grassland	1.1	1.1	0.95	1,544	1 Jan – 30 Jun 2002
Paddy rice field	1.0	1.0	1.0	857	26 Sep – 31 Dec 2006
Forest	1.25	1.5	1.7	1,135	1 Apr – 31 Dec 2005
Average	1.12	1.20	1.22		

C_T , C_q and C_{CO_2} were determined by Eqs. (2), (3), and (4), respectively. With Eq. (2), linear regression was applied between measured σ_T/T^* and $(-z-d)/L)^{-1/3}$ to determine C_T . The constants C_q and C_{CO_2} were determined with same procedure.

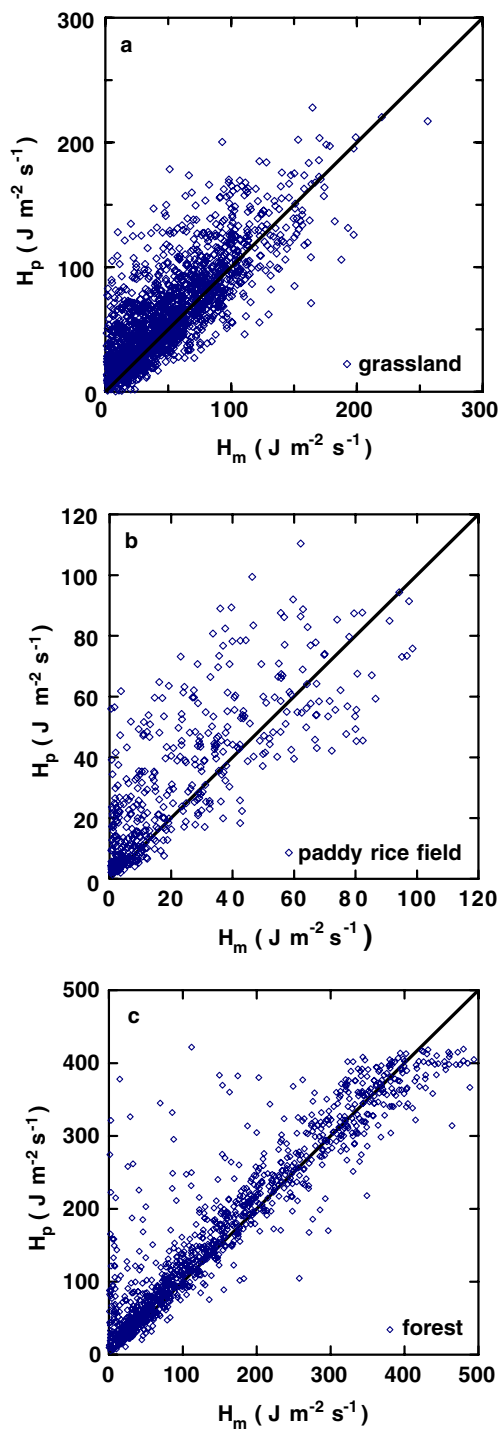


Fig. 10 Comparisons of eddy-covariance measured (H_m) and flux-variance predicted (H_p) sensible heat fluxes for **a** grassland, **b** rice paddy field, and **c** forest. The 1:1 line is also shown

standard deviation of temperature (σ_T/T^*) as a function of the stability parameter, ζ , for the three sites: (a) grassland, (b) paddy rice field, and (c) forest. Figure 8 is the same as Fig. 7 but for water vapor (σ_q/q^*). The $-1/3$ power law is evident in both Figs. 7 and 8. Notice that, in Fig. 8b, under

neutral condition ($0.001 < -(z-d)/L < 0.01$), due to the strong evapotranspiration from the flooded rice paddy, the flux-variance relationship for the water vapor is close to a constant. In Fig. 4, the similarity constants of temperature (C_T) for the grassland, rice paddy, and forest are 1.1, 1.0, and 1.25, respectively. From the literature, the value for C_T has been found to vary between 0.95 and 1.36 (Ohtaki 1985; Wesely 1988; Katul et al. 1995; Hsieh et al. 1996; Gao et al. 2006). In Fig. 8, the similarity constants of humidity (C_q) for the grassland, rice paddy, and forest are 1.1, 1.0, and 1.5, respectively. In the past, C_q has been found to vary between 1.1 and 1.5 (Ohtaki 1985; Wesely 1988; Lamaud and Irvine 2006; Gao et al. 2006). Note that the values of C_T and C_q in our study were within these ranges.

Figure 9 is the same as Fig. 7 but for carbon dioxide (σ_{CO_2}/CO_{2*}). In Fig. 9, although some of the data follow the $-1/3$ power law, the scatters spread out for all the three sites and the flux-variance relations are not as good as those for temperature and water vapor. The R^2 values for Fig. 9a to c are only 0.21, 0.26, and 0.50, respectively. The similarity constants of CO_2 (C_{CO_2}) for the grassland, paddy rice field, and forest were 0.95, 1.0 and 1.7, respectively. It is worth noting that our value of C_{CO_2} for the paddy rice field was consistent with Ohtaki's (1985) experiment which suggests that $C_{CO_2}=1.1$ for free convection conditions above a rice paddy. Moreover, the constant for the grassland is close to Detto and Katul's (2007) value ($C_{CO_2}=0.99$) for a grass-covered surface. The similarity constants for heat, water vapor, and CO_2 for the three sites are summarized in Table 2. Here, C_T , C_q and C_{CO_2} were determined by Eqs. (2), (3), and (4), respectively. With Eq. (2), linear regression was applied between measured σ_T/T^* and $-(z-d)/L$ to determine C_T . The constants C_q and C_{CO_2} were determined with same procedure.

From Figs. 7, 8 and 9, we found that, for the grassland and forest sites, temperature follows the flux-variance relation better than humidity does. This better flux-variance relation for temperature for the same site has been found in the past (see reviews in Moriwaki and Kanda 2006) and attributed to the less homogeneity of water vapor sources/sinks distribution. However, different from the literature, it is the reverse for our paddy rice field. This is attributed to the fact that the sources/sinks distribution of water vapor is more homogeneous than that for temperature since this rice paddy field was uniformly irrigated and flooded with water. This indicates that, for the same site, the temperature flux-variance relationship is not always better than the humidity one; it depends on the sources/sinks distribution on the site.

Also, from Figs. 7, 8 and 9, for small roughness surfaces like grassland and rice paddy, the similarity constants for different scalars are all around 1.0, but for

Table 3 Coefficients of regression analyses between measured and estimated sensible heat (H), water vapor (LE), and CO₂ fluxes

Ecosystem	Flux	Slope	Intercept	R ²	SEE
Grassland					
No. of data points: 1,737; period: 1 Jul 2002 – 31 Dec 2006	H (J m ⁻² s ⁻¹)	0.83	20.31	0.64	23.91
	LE (J m ⁻² s ⁻¹)	0.79	28.5	0.60	37.5
	LE (J m ⁻² s ⁻¹) with measured H	0.81	16.79	0.70	31.58
	CO ₂ flux (mmol m ⁻² s ⁻¹)	0.56	0.0073	0.16	0.0067
	CO ₂ flux (mmol m ⁻² s ⁻¹) with measured H	0.63	0.0056	0.23	0.0059
Paddy rice field					
No. of data points: 454; period: 1 Jan 2006 – 18 May 2007	H (J m ⁻² s ⁻¹)	0.79	13.17	0.60	15.03
	LE (J m ⁻² s ⁻¹)	0.74	16.09	0.78	31.06
	LE (J m ⁻² s ⁻¹) with measured H	0.79	1.69	0.88	23.73
	CO ₂ flux (mmol m ⁻² s ⁻¹)	0.6	0.0064	0.07	0.0077
	CO ₂ flux (mmol m ⁻² s ⁻¹) with measured H	0.68	0.0042	0.24	0.0043
Forest					
No. of data points: 1,237; period: 1 Jan – 31 Dec 2006	H (J m ⁻² s ⁻¹)	0.88	35.02	0.87	43.72
	LE (J m ⁻² s ⁻¹)	0.9	53.21	0.61	76.16
	LE (J m ⁻² s ⁻¹) with measured H	0.85	45.66	0.64	67.03
	CO ₂ flux (mmol m ⁻² s ⁻¹)	0.61	0.0085	0.42	0.0046
	CO ₂ flux (mmol m ⁻² s ⁻¹) with measured H	0.71	0.0064	0.54	0.0042

rough surfaces like forest, the similarity constants are larger. For understanding the roles of these similarity constants, we consider the relative transport efficiency of sensible heat to water vapor, λ_{Tq}, calculated as (McBean and Miyake 1972)

$$\lambda_{Tq} = \frac{R_{wT}}{R_{wq}} = \frac{\overline{w'T'} / (\sigma_w \sigma_T)}{\overline{w'q'} / (\sigma_w \sigma_q)} = \frac{\overline{w'T'} \sigma_q}{\overline{w'q'} \sigma_T} \tag{8}$$

where R_{wT} and R_{wq} are the correlation coefficients between W and T and W and q, respectively. In Eq. (8), if we substitute σ_T with Eq. (2) and σ_q with Eq. (3), we can then get

$$\lambda_{Tq} = \frac{R_{wT}}{R_{wq}} = \frac{C_q}{C_T} \tag{9}$$

Equation (9) describes that the ratio of C_q to C_T is in fact the average relative transport efficiency of sensible heat to latent heat fluxes for the same site. With a similar derivation, the ratio of C_{CO₂} to C_T can be found to be the average relative transport efficiency of sensible heat to carbon dioxide fluxes if CO₂ follows the flux-variance relationship. For the grassland and paddy rice ecosystems, the three similarity constants for heat, water vapor, and CO₂ are almost the same, which indicates that water vapor and carbon dioxide are transported as efficiently as heat in these two sites. For the forest ecosystem, C_q/C_T=1.2 and C_{CO₂}/C_T=1.36 indicate that water vapor and carbon dioxide are transported 20–36% less efficiently than heat. However, it should be kept in mind that CO₂ does not follow MOST flux-variance relation for the three sites.

Estimations of sensible heat, latent heat, and CO₂ fluxes

With Eq. (5) to (7) and measured standard deviations of temperature, water vapor, and carbon dioxide, we estimated the surface fluxes for the three ecosystems. Figure 10 shows the comparisons of sensible heat flux between eddy-covariance measurements and flux-variance predictions over the three sites: (a) grassland, (b) paddy rice field, and (c) forest. Reasonable agreements between measured and predicted sensible heat fluxes are found in Fig. 10 for all the three sites. The R² values are between 0.60 to 0.87 (see Table 3 for details). Note that the standard errors of estimation (SEE) are around 15–40 W m⁻² for the three sites. This finding is similar to Michiaki and Noriaki's (2003) result which concludes that the SEE of estimated H by the flux-variance method is about 20 W m⁻² in the atmospheric surface layer.

Figure 11 is the same as Fig. 10 but for latent heat flux. Reasonable agreements between the measured and predicted latent heat fluxes are shown in Fig. 11 for all the three sites. The R² values for the three sites are between 0.60 and 0.78. Note that the performance of using flux-variance method for the LE predictions is better than the H predictions for the rice paddy. This result is surprising and is different from other literature results (e.g., Weaver 1990; Katul et al. 1995; Moriwaki and Kanda 2006).

In the past, the reason for a worse LE prediction by the flux-variance method has been attributed to the less uniformity of LE sources and sinks when compared to H (e.g., Weaver 1990; Padro 1993; Katul et al. 1995).

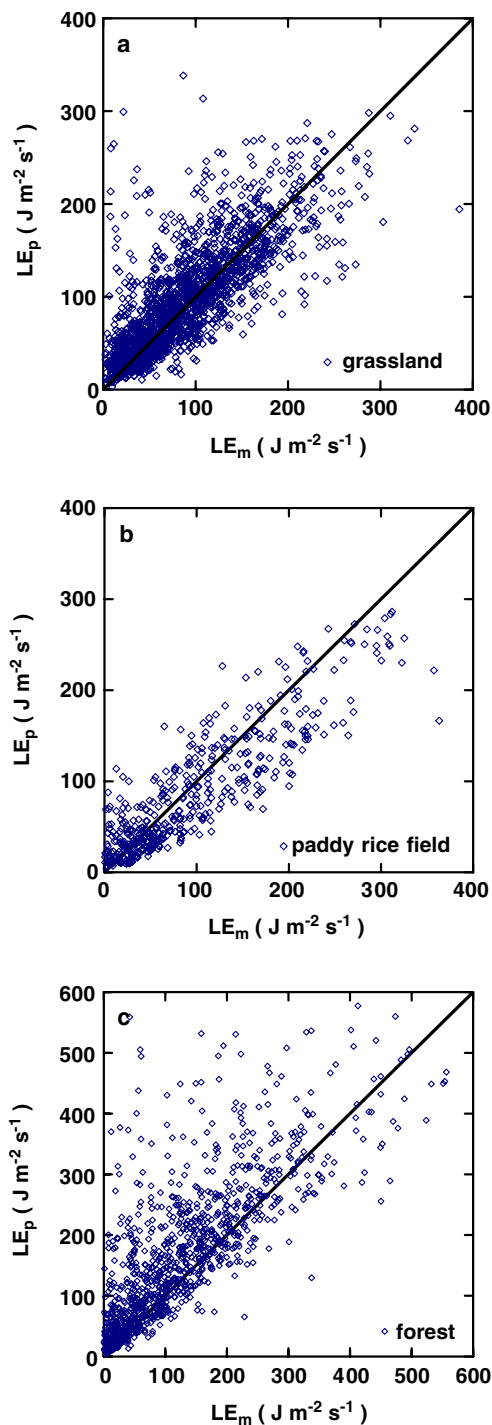


Fig. 11 Comparisons of eddy-covariance measured (LE_m) and flux-variance predicted (LE_p) water vapor fluxes for **a** grassland, **b** rice paddy field, and **c** forest. The 1:1 line is also shown

However, if we rearrange Eq. (3) and substitute L with its definition, we then have

$$LE = L_v \frac{\sigma_q}{C_q} \left(k(z-d) \frac{g}{\rho C_p T} H \right)^{1/3} \quad (10)$$

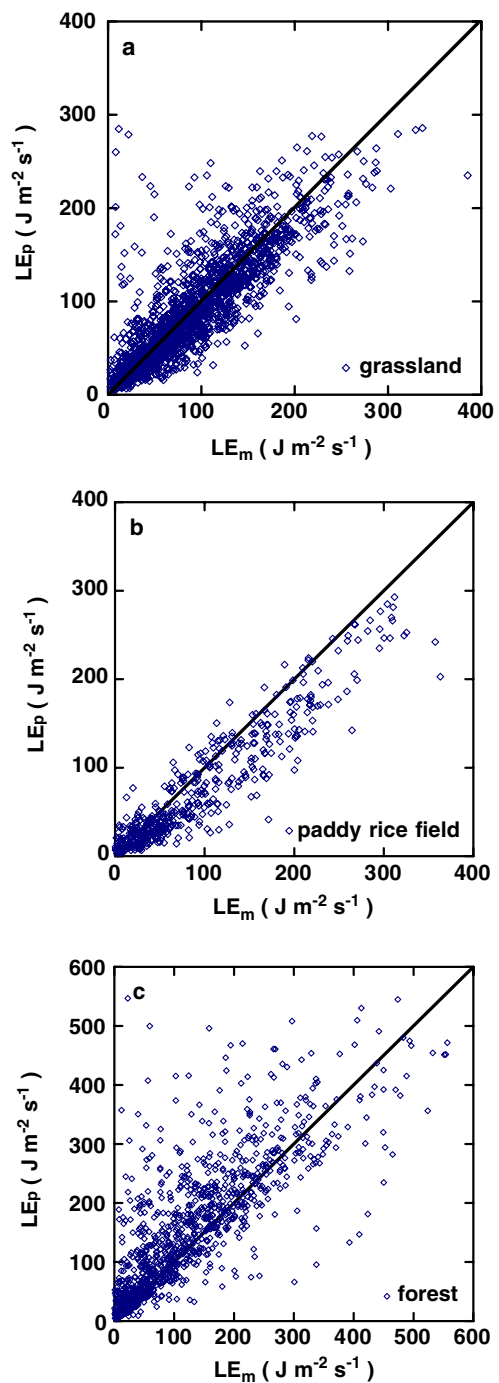


Fig. 12 Comparisons of eddy-covariance measured (LE_m) and flux-variance predicted (LE_p) water vapor fluxes for **a** grassland, **b** rice paddy field, and **c** forest with LE_p estimated by Eq. (10) with measured sensible heat flux. The 1:1 line is also shown

It is clear, from Eq. (10), the accuracy of LE estimation also depends on H (i.e., the uncertainty of H will influence the accuracy of LE prediction). In Eq. (10) if H is estimated by Eq. (5), then Eq. (10) is reduced to Eq. (6) (i.e., combining Eq. (10) and (5) we will have Eq. (6)). With eddy-covariance measured H and σ_q , we used Eq. (10) to predict LE for the three sites. The comparisons between LE

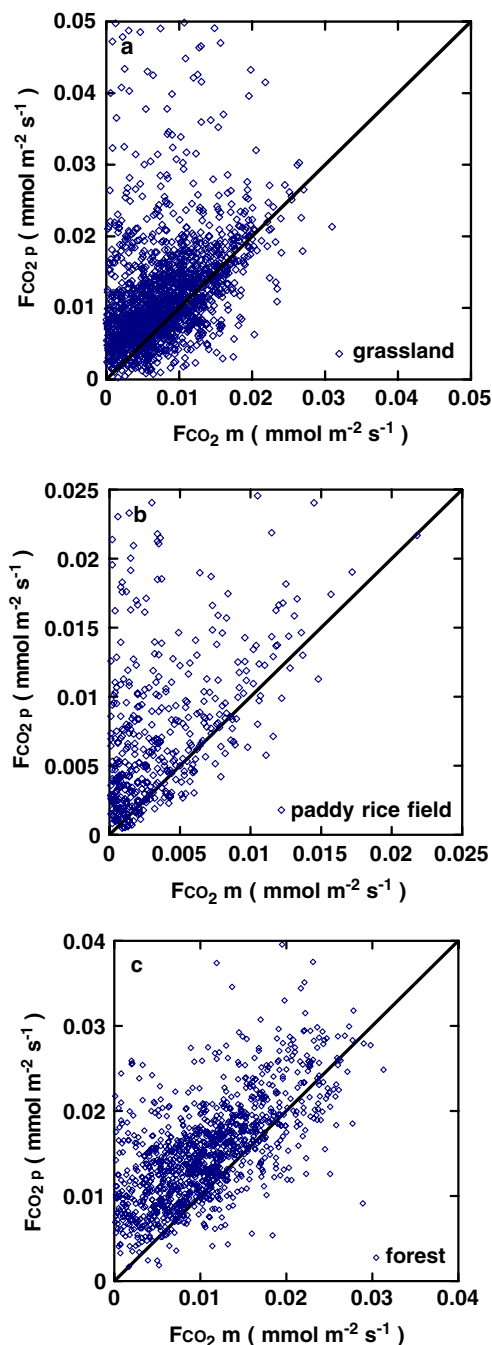


Fig. 13 Comparisons of eddy-covariance measured (F_{CO_2m}) and flux-variance predicted (F_{CO_2p}) CO_2 fluxes for **a** grassland, **b** rice paddy field, and **c** forest. The 1:1 line is also shown

measurements and predictions are shown in Fig. 12. It is evident that the LE estimations are improved if Eq. (10) is adopted (with measured H) instead of Eq. (6). For the grassland site, the R^2 for LE is improved from 0.60 to 0.70 and, for the paddy rice field, it is raised from 0.78 to 0.88. For the forest, the R^2 is improved from 0.61 to 0.64. The

regression statistics between the measured and predicted fluxes are summarized in Table 3.

From the above discussion, it is worth noting that the flux-variance method can predict a better LE if H is given correctly. This means that, for the same field site, it is not always the case that surface heating (sensible heat sources/sinks) is more homogeneous than surface evapotranspiration (water vapor sources/sinks). Also, in this study, our results show that for the paddy rice field water vapor sources/sinks are more homogeneous than those for sensible heat.

Figure 13 shows the comparisons between the eddy-covariance measured and the flux-variance method predicted CO_2 fluxes for the three sites. The results are not as good as those for H and LE, especially for the paddy rice field. The R^2 values in Fig. 13 are 0.16, 0.07, and 0.42 for the grassland, paddy rice, and forest, respectively.

Similarly to the derivation for LE, if we rearrange Eq. (4) and substitute L with its definition, we then have

$$F_{CO_2} = \frac{\sigma_{CO_2}}{C_{CO_2}} \left(k(z-d) \frac{g}{\rho C_p T} H \right)^{1/3} \quad (11)$$

By Eq. (11), it is clear the accuracy of CO_2 flux estimation also depends on H (i.e., the uncertainty of H will influence the accuracy of F_{CO_2} prediction). In Eq. (11) if H is estimated by Eq. (5), then Eq. (11) is reduced to Eq. (7) (i.e., combining Eq. (11) and (5) we will have Eq. (7)). With eddy-covariance measured H and σ_{CO_2} , we used Eq. (11) to predict CO_2 flux for the three ecosystems. The comparisons between CO_2 flux measurements and predictions are shown in Table 3. It is obvious that the F_{CO_2} estimations are improved if Eq. (11) is adopted (with measured H) instead of Eq. (7). For the grassland site, the R^2 for CO_2 flux is improved from 0.16 to 0.23. For the grassland and forest, the values are raised from 0.07 to 0.24 and 0.42 to 0.54, respectively.

All the above statistics were summarized in Table 3. From Table 3, it is clear that CO_2 flux does not follow MOST. This finding is consistent with Detto and Katul's (2007) result. We attribute this to the complicated distribution of CO_2 sources/sinks on the surface and its changes with seasons (Williams et al. 2007). For CO_2 , this distribution of sources/sinks is mainly controlled by the vegetation, biochemistry activities in the soil, and field management (e.g., fertilization).

Conclusions

This study examined the flux-variance relations of temperature, water vapor and CO_2 and the performance of the

flux-variance method for predicting sensible heat, latent heat, and CO₂ fluxes. Our results suggest the following:

1. The flux-variance relations (or the similarity constants) for temperature, humidity, and CO₂ has to be determined a priori before using the flux-variance method for predicting sensible heat, latent heat, and CO₂ fluxes. However, if the determination of the flux-variance relation is not possible for the field site, then the values around 1.0 for both C_T and C_q is recommended for short vegetation surfaces.
2. For all the three ecosystems, the flux-variance method predictions of H and LE are in reasonable agreement with eddy-covariance measurements. And if the LE predictions were obtained in conjunction with measured sensible heat flux, the prediction accuracy could be improved by around 15 percent.
3. Due to the complicated carbon dioxide sources/sinks distribution, the CO₂ flux-variance relation does not follow MOST. The CO₂ predictions were found to be between poor and fair among the three sites.
4. For the irrigated paddy rice field, our results showed that surface sources/sinks for water vapor were more homogeneous than those for sensible heat. Hence, the latent heat flux predictions by the flux-variance method were better than the sensible heat flux ones.
5. For the grassland and rice paddy, water vapor was transported as efficient as heat. For the forest, heat transport efficiency was 20% higher than water vapor.

Acknowledgments The authors would like to thank the National Science Council and Environmental Protection Agency, Taiwan, for their support of this study. We are also very grateful to Professor Gerard Kiely for his data support and the two reviewers for their helpful comments.

References

- Andreas EL, Hill RJ, Gosz JR, Moore DI, Otto WD, Sarma AD (1998) Statistics of surface layer turbulence over terrain with meter-scale heterogeneity. *Boundary-Layer Meteorol* 86:379–408
- Asanuma J, Brutsaert W (1999) Turbulence variance characteristics of temperature and humidity in the unstable atmospheric surface layer above a variable pine forest. *Water Resour Res* 35:2281–2288
- Campbell GS, Norman JM (1998) An introduction to environmental biophysics, 2nd edn. Springer, New York
- Castellvi F, Martinez-Cob A (2005) Estimation sensible heat flux using surface renewal analysis and the flux variance method: a case study over olive trees at Sastago (NE of Spain). *Water Resour Res* 41:W09422
- de Bruin HAR, Kohsiek W, Van Den Hurk BJM (1993) A verification of some methods to determine the fluxes of momentum, sensible heat, and water vapor using standard deviation and structure parameter of scalar meteorological quantities. *Boundary-Layer Meteorol* 63:231–257
- Detto M, Katul GG (2007) Simplified expressions for adjusting higher-order turbulent statistics obtained from open path gas analyzers. *Boundary-Layer Meteorol* 122:205–216
- Gao Z, Bian L, Chen Z, Sparrow M, Zhang J (2006) Turbulent variance characteristics of temperature and humidity over a non-uniform land surface for an agriculture ecosystem in China. *Adv Atmos Sci* 23:365–374
- Hsieh CI, Katul GG, Sigmon J, Knoerr KR (1996) Estimation of momentum and heat fluxes using dissipation and flux-variance methods in the unstable surface layer. *Water Resour Res* 32:2453–2462
- Hsieh CI, Katul GG, Chi TW (2000) An approximate analytical model for footprint estimation of scalar fluxes in thermally stratified atmospheric flows. *Adv Water Resour* 23:765–772
- Hsieh CI, Kiely G, Birkby A, Katul G (2005) Photosynthetic responses of a humid grassland ecosystem to future climate perturbations. *Adv Water Resour* 28:910–916
- Jaksic V, Kiely G, Albertson J, Oren R, Katul G, Leahy P, Byrne KA (2006) Net ecosystem exchange of grassland in contrasting wet and dry years. *Agri For Meteorol* 139:323–334
- Katul GG, Goltz M, Hsieh C, Cheng Y, Mowry F, Sigmon J (1995) Estimation of surface heat and momentum fluxes using the flux-variance method above uniform and non-uniform terrain. *Boundary-Layer Meteorol* 74:237–260
- Lamaud E, Irvine M (2006) Temperature-humidity dissimilarity and heat-to-water vapor transport efficiency above and within a pine forest canopy: the role of the Bowen ratio. *Boundary-Layer Meteorol* 120:87–109
- Lloyd CR, Culf AD, Dolman AJ, Gash JH (1991) Estimates of sensible heat flux from observations of temperature fluctuations. *Boundary-Layer Meteorol* 57:311–322
- McBean GA, Miyake M (1972) Turbulent transfer mechanisms in the atmospheric surface layer. *Quart J R Meteorol Soc* 98: 383–398
- McMillen R (1988) An eddy correlation technique with extended applicability to non-simple terrain. *Boundary-Layer Meteorol* 43:231–245
- Michiaki S, Noriaki K (2003) Surface and mixed-layer variance methods to estimate regional sensible heat flux at the surface. *Boundary-Layer Meteorol* 106:117–145
- Moore CJ (1986) Frequency response corrections for eddy correlation systems. *Boundary-Layer Meteorol* 37:17–35
- Moriwaki M, Kanda M (2006) Local and global similarity in turbulent transfer of heat, water vapor, and CO₂ in the dynamic convective sublayer over a suburban area. *Boundary-Layer Meteorol* 120:163–179
- Ohtaki E (1985) On the similarity in atmospheric fluctuations of carbon dioxide, water vapor and temperature over vegetated fields. *Boundary-Layer Meteorol* 32:25–37
- Padro J (1993) An investigation of flux-variance methods and universal functions applied to three land-use types in unstable conditions. *Boundary-Layer Meteorol* 66:413–425
- Tillman JE (1972) The indirect determination of stability, heat and momentum fluxes in the atmosphere boundary layer from simple scalar variables during dry unstable conditions. *J Appl Meteorol* 44:13–31

- Weaver HL (1990) Temperature and humidity flux-variance relations determined by one-dimensional eddy correlations. *Boundary-Layer Meteorol* 53:77–91
- Webb EK, Perman GI, Leuning R (1980) Correction of flux measurements for density effects due to heat and water transfer. *Quart J R Meteorol Soc* 106:85–100
- Wesely ML (1988) Use of variance techniques to measure dry air-surface exchange rates. *Boundary-Layer Meteorol* 44:13–31
- Wesson KH, Katul GG, Lai CT (2001) Sensible heat flux estimation by flux variance and half-order time derivative methods. *Water Resour Res* 37:2333–2343
- Wilczak JM, Oncley SP, Stage SA (2001) Sonic anemometer tilt correction algorithms. *Boundary-Layer Meteorol* 99:127–150
- Williams CA, Scanlon TM, Albertson JD (2007) Influence of surface heterogeneity on scalar dissimilarity in the roughness sublayer. *Boundary-Layer Meteorol* 122:149–165